Nuclear Materials and Energy 15 (2018) 13–16

Contents lists available at ScienceDirect

Nuclear Materials and Energy

journal homepage: www.elsevier.com/locate/nme

Ion irradiation effects on FeCrAl-ODS ferritic steel

K. Kondo[a,*], S. Aoki[a], S. Yamashita[a], S. Ukai[b], K. Sakamoto[c], M. Hirai[c], A. Kimura[d]

[a] Japan Atomic Energy Agency, Tokai-mura, Naka-gun, Ibaraki-ken 319-1195, Japan
[b] Hokkaido University, Kita 8 nishi 5, Kita-ku, Sapporo-shi, Hokkaido 060-0808, Japan
[c] Nippon Nuclear Fuel Development Co., Ltd, Narita-cho, Oarai-machi, Higashi-ibaraki-gun, Ibaraki-ken 311-1313, Japan
[d] Kyoto University, Gokasyo, Uji 611-011, Japan

ABSTRACT

The correlation between microstructure and mechanical property of ion irradiated 12Cr-6Al ODS ferritic steel was studied. Ion irradiation experiments were performed using 10.5 MeV Fe ions up to the nominal displacement damage of 20 dpa with the damage rate of 1×10^{-4} dpa/s, while the irradiation temperature was 300 °C. Oxide nanoparticles showed stable size distribution and mean size under ion irradiation up to 20 dpa. The irradiation microstructure examined by TEM revealed that the mean size and number densities of irradiation-induced defect clusters increased with the displacement damage. The correlation between irradiation microstructure and radiation hardening was theoretically calculated using the dispersed barrier hardening model. The results showed a good agreement with the experimentally measured hardness data up to irradiation at 5 dpa, while a slight discrepancy was found between theoretical and experimental hardness values under irradiation at 20 dpa. Radiation hardening in 12Cr-6Al ODS ferritic steel was mainly caused by irradiation-induced defect clusters below the irradiation dose of 5 dpa. As the irradiation dose increased toward 20 dpa, an additional influence of the radiation appeared, which was assumed to be induced by α' phase transformation.

1. Introduction

With the growing interest in oxide dispersion strengthened (ODS) ferritic/martensitic and ferritic steels utilized to various nuclear applications, extensive research on those steels have revealed their strength at high temperature and microstructural stability under irradiation conditions. Therefore, it is widely recognized that ODS steels are adequate as a structural material for the fusion blanket exposed to extremely severe conditions, such as elevated temperature, neutron irradiation and corrosive environment caused by solid breeder and coolant. And, the optimization of solute content in ODS steels has also been made for the purpose of improving mechanical, chemical and irradiation resistant properties, enabling the withstanding at high operating temperature of fusion reactors.

This study focuses on the development of ODS ferritic steels with the combination of irradiation resistance and corrosion property. The concept of the alloy design is as follows. Chromium is well-known as a solute element to improve heat and corrosion resistance of steels. ODS ferritic steels with a high chromium content often experiences the formation of Cr rich α' phase by thermal aging at above 400 °C [1] or by irradiation at a low temperature [2]. In order to reduce the formation of brittle Cr rich α' phase under irradiation at elevated temperature, chromium content of the alloy should be set as low as possible. Although the corrosion resistance is reduced by the decrease in chromium content, it could be compensated by addition of aluminum in the matrix of ODS ferritic steels. The advantageous effect of aluminum on the corrosion property of ODS ferritic steels was reported by Kimura et al., and the mechanisms was explained by the formation of stable Al_2O_3 oxide layer together with the $(Cr, Fe)_2O_3$ layer [3,4]. As far as the aluminum addition was concerned, however, adverse effects were also reported. For example, Isselin et al. reported the enhancement of embrittlement by aluminum doped in high Cr ODS ferritic steels after aging at 450 °C [5], also suggesting the need to optimize Cr and Al contents of steels. Furthermore, phase stability of matrix [1], composition and chemical property of oxide nanoparticle after the fabrication process [6], and compatibility with aluminum containing matrix, especially recoil dissolution of oxides [7] should also be concerns of aluminum doped ODS ferritic steels.

In this study, based on the consideration mentioned above, 12Cr-6Al ODS ferritic steel was produced. The present paper reports the fundamental irradiation effect on the mechanical property and related microstructural evolution in the 12Cr-6Al ODS ferritic steel.

* Corresponding author.
E-mail address: kondo.keietsu@jaea.go.jp (K. Kondo).

https://doi.org/10.1016/j.nme.2018.05.022
Received 15 December 2017; Received in revised form 5 April 2018; Accepted 24 May 2018
Available online 01 June 2018

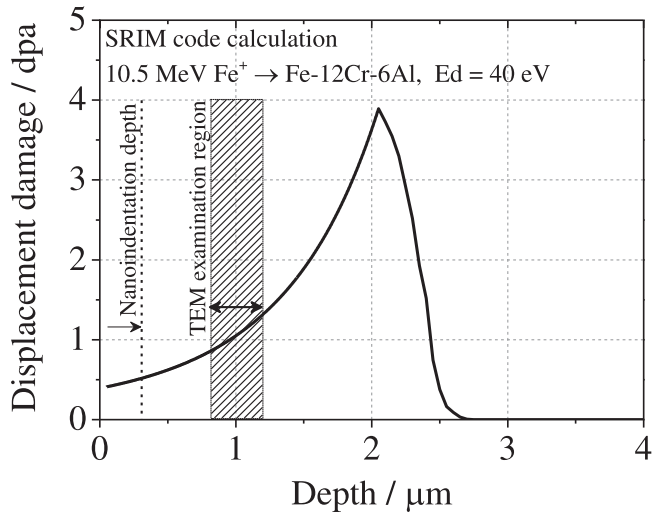

Fig. 1. 10.5 MeV Fe ion irradiation up to the irradiation dose of 1 dpa at the depth of 1 μm.

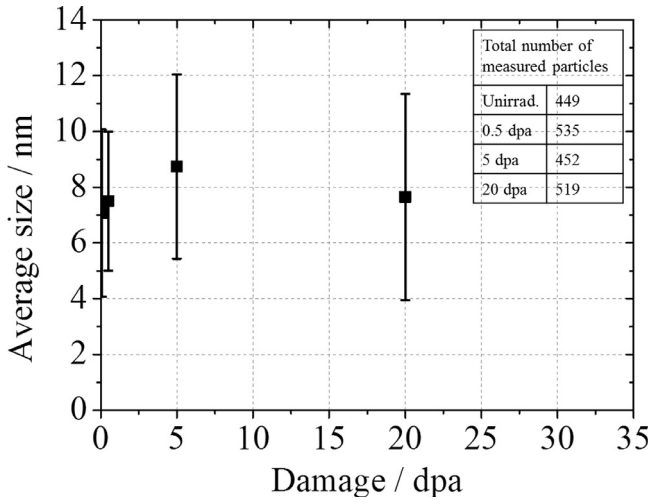

Fig. 2. Irradiation dose dependence on the mean size of nanoparticles in 12Cr-6Al ODS ferritic steel.

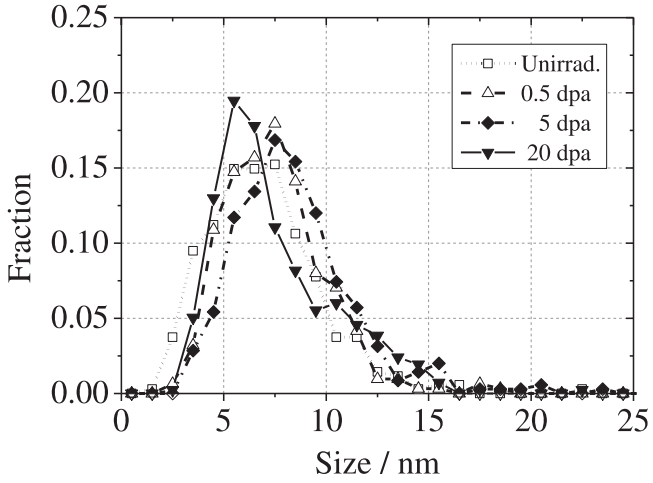

Fig. 3. Size distribution of nanoparticles in ion irradiated 12Cr-6Al ODS ferritic steel.

2. Experimental

Test material used in this study was 12Cr-6Al ODS ferritic steel, manufactured with the mechanical alloying process and subsequent hot extrusion at 1150 °C. Its chemical compositions were Fe-12Cr-6Al-0.4Zr-0.5Ti-0.5Y_2O_3-0.24Ex.O.

Prior to the irradiation experiment, specimens were mechanically polished using SiC abrasive papers, and then electro-polished to remove the work hardened layer. Ion irradiation experiments using 10.5 MeV Fe^+ ion was carried out at Takasaki Ion Accelerators for Advanced Radiation Application Facility in National Institutes for Quantum and Radiological Science and Technology. Irradiation temperature was controlled as 300 °C. Fig. 1 shows the result of the SRIM code calculation [8] for the depth profile of the displacement damage using the threshold displacement energy of 40 eV for iron. In this study, displacement damage at the depth of 1 μm was adopted as the nominal displacement damage of the irradiated specimen, which were selected to be 0.5, 5, and 20 dpa. The damage rate was approximately 1×10^{-4} dpa/s.

The microstructural characterization was carried out after ion irradiation to various damage levels. Thin foil specimens for TEM observation were fabricated by focused Ga-ion beam milling with NB-5000 Hitachi FIB/SEM operated at a voltage of 40 kV. Subsequent flash electro-polishing was also conducted with the electrolyte which contains 2% perchloric acid and 98% methanol at the temperature below −50 °C in order to remove the FIB induced damage. TEM observation on the microstructure at 1 μm depth from the irradiated surface was performed using HF-3300 Hitachi FEG-TEM operated at an acceleration voltage of 300 kV.

The mechanical property of irradiated specimens was measured using the nanoindenter (Elionix ENT-1100b) with a Berkovich tip. Considering the plastic zone size during indentation loading, the indentation depth was controlled to be approximately 0.3 μm in order to estimate the hardness of the irradiated surface region to the depth of 1 μm.

3. Results and discussion

3.1. Stability of oxide nanoparticles

The stability of oxide nanoparticles under ion irradiation was examined by TEM observation on the ion irradiated 12Cr-6Al ODS ferritic steels. Figs. 2 and 3 show the dose dependence of mean size and size distribution of nanoparticles, respectively. Taking the standard deviation into consideration, mean size of nanoparticles was not influenced significantly by ion irradiation (Fig. 2). In addition, the size distribution of nanoparticles was not changed by ion irradiation, as shown in Fig. 3. Those results suggest that nanoparticles in the matrix of 12Cr-6Al ferritic steel didn't undergo drastic dissolution or coarsening, since the evident change in nanoparticles was not be observed under the irradiation condition in this study.

3.2. Irradiation microstructure

Fig. 4 shows the microstructure in 12Cr-6Al ODS ferritic steel before and after irradiation. The bright field image shown in Fig. 4 was taken under the condition of g = 110 with beam direction close to z = 001 [9]. The network dislocations with the low density were mainly observed before irradiation. Irradiation microstructure of the 0.5 dpa-irradiated specimens was dominated with black dot defects with sizes from 2 to 4 nm. Above 5 dpa irradiation, dislocation loops were observed and their size became larger with dose. According to literatures for irradiation-induced defects [10], those black dots and dislocation loops are presumed to be predominantly a[100] type, and the low density of a/2[111] type might exist. Size distribution of irradiation-induced defect clusters in each irradiation dose level is shown in Fig. 5, and the mean size and number density of observed defects are summarized in Table 1. The thickness of TEM foil specimens was

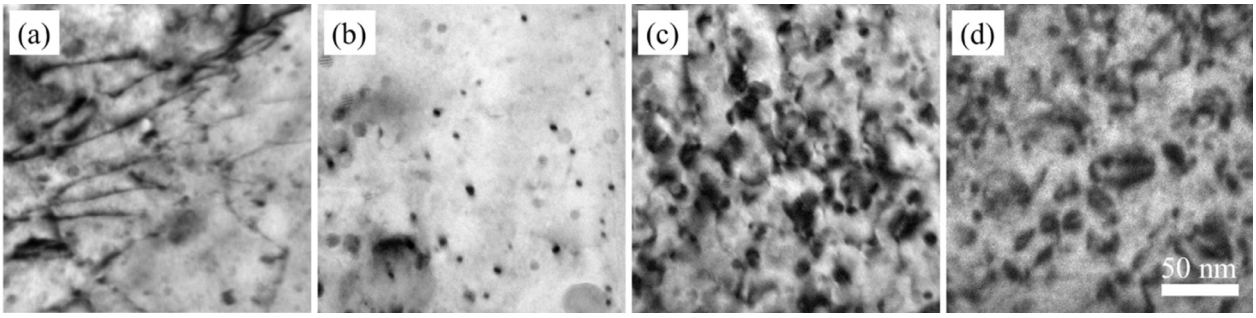

Fig. 4. Dislocation microstructure in 12Cr-6Al ODS ferritic steels (a) before irradiation, and after irradiation up to (b) 0.5, (c) 5, and (d) 20 dpa, respectively.

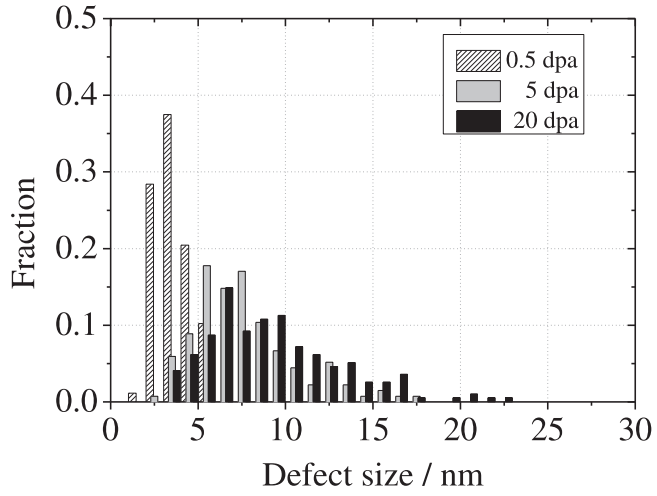

Fig. 5. Size distributions of defect clusters in ion irradiated 12Cr-6Al ODS steels.

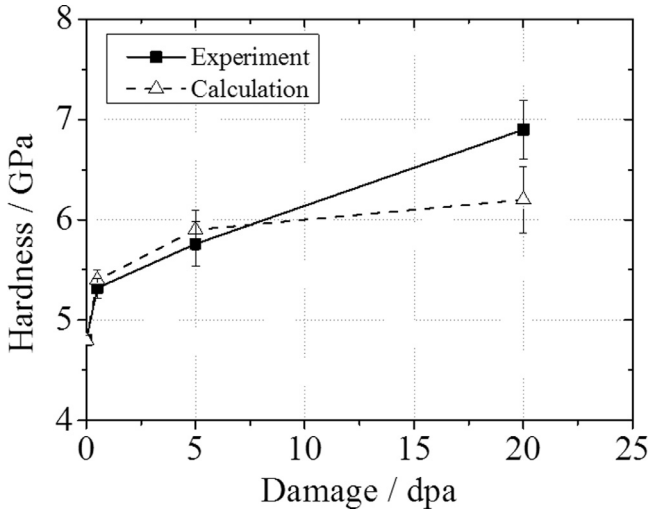

Fig. 6. Radiation hardening behavior in Fe^{+} ion irradiated 12Cr-6Al ODS ferritic steel. Solid line is the experimental data, and dashed line is the calculation result.

Table 1
The mean size and number density of the irradiation-induced defect clusters.

Damage / dpa	Mean size / nm	Number density / m^{-3}
0.5	3.7	8.3×10^{21}
5	7.6	1.2×10^{22}
20	9.6	2.5×10^{22}

determined using thickness fringes observed on inclined grain boundaries under the exact Bragg condition. The distribution of defect cluster size is shifted toward the large size side with increasing the irradiation dose, resulting in the increase in the mean size of defects. Besides, the defect density tended to increase with the irradiation dose within the irradiation condition in this study.

3.3. Radiation hardening

The radiation hardening behavior experimentally obtained by nanoindentation testing is shown in Fig. 6 (solid line). Nanoindentation hardness before irradiation was 4.8 GPa, and Fe-ion irradiation to 0.5 dpa caused the radiation hardening up to 5.3 GPa. The hardness values further increased with the irradiation dose at 5 dpa and reached 6.6 GPa at 20 dpa. In order to estimate the amount of radiation hardening caused by the defect clusters induced by radiation, theoretical calculations were carried out by applying the results of TEM observation to the dispersed barrier hardening model expressed by the following Eq. (1) [11,12]:

$$\Delta\sigma = \alpha\mu \mathrm{Mb}\,(\Delta \mathrm{Nd})^{1/2}, \quad (1)$$

where, $\Delta\sigma$ is the increase of yield strength. Other material parameters in the equation are dislocation-defect interaction strength $\alpha = 0.5$, shear modulus $\mu = 82$ GPa, Taylor factor $M = 3.06$, burgers vector of the dislocation $b \sim 0.25$ nm, and the number density and mean size of defect clusters induced by irradiation, N and d, respectively [12]. In this study, because the hardness of irradiated 12C-6Al ODS steels was estimated by means of nanoindentation testing (ΔH_N), calculated yield stress ($\Delta\sigma$) was converted to vickers hardness (ΔH_V) and, furthermore, nanoindentation hardness (ΔH_N) by following Eqs. (2) and (3) suggested by Busby et al. [13] and Oliver and Pharr [14], respectively.

$$\Delta\sigma = 3.06\,\Delta \mathrm{H_V} \quad (2)$$

$$\Delta \mathrm{H_V} = 94.59\,\Delta \mathrm{H_N} \quad (3)$$

The calculated radiation hardening behavior is shown in Fig. 6 with a dashed line, while the experimental data of 4.8 GPa was employed as the hardness before irradiation. As shown in Fig. 6, the calculated hardness values were in good agreement with experimental values up to 5 dpa, suggesting that the hardening was mainly caused by irradiation-induced defect clusters within this dose range. In case of irradiation dose below 20 dpa, on the other hand, the experimental value was slightly larger than the calculation one, implying the existence of another hardening factor in addition to irradiation-induced defect clusters. Briggs [3] reported results of three dimensional atom probe analysis on Al doped ODS ferritic steel. The formation of α' phase occurred after neutron irradiation up to the dose of 7 dpa at the irradiation temperature ranged from 320 to 382 °C. Therefore, it is considered that the formation of fine α' phase occurred in 12Cr-6Al ODS ferritic steel after Fe-ion irradiation up to 20 dpa, which caused radiation hardening together with the matrix radiation damages. Further investigation by three dimensional atom probe is required to reveal the occurrence of α'

phase transformation and its contribution to hardening of ion irradiated 12Cr-6Al ODS ferritic steel.

4. Summary

Assessment of irradiation effects on the microstructural evolution and the consequent mechanical property in 12Cr-6Al ODS ferritic steel was carried out using Fe ion irradiation at the irradiation temperature of 300 °C.

1. Oxide nanoparticles in 12Cr-6Al ferritic steel showed the good structural stability under ion irradiation up to 20 dpa.
2. A correlation between irradiation microstructure and radiation hardening was theoretically calculated by applying the results of TEM examination to the dispersed barrier hardening model. The results showed a good agreement with the experimentally obtained hardness data up to 5 dpa irradiation. A slight discrepancy was found between theoretical and experimental values of 20 dpa irradiation.
3. Radiation hardening in 12Cr-6Al ODS ferritic steel was mainly caused by the irradiation defect clusters up to the irradiation dose of 5 dpa. It was considered that, with increasing the irradiation dose toward 20 dpa, the effect of formation of α' phase on the hardening might appear.

Acknowledgement

This study is the result of "Development of Technical Basis for Introducing Advanced Fuels Contributing to Safety Improvement of Current Light Water Reactors" carried out under the Project on Development of Technical Basis for Safety Improvement at Nuclear Power Plants by Ministry of Economy, Trade and Industry (METI) of Japan.

Supplementary materials

Supplementary material associated with this article can be found, in the online version, at doi:10.1016/j.nme.2018.05.022.

References

[1] J.S. Lee, C.H. Jang, I.S. Kim, A. Kimura, Embrittlement and hardening during thermal aging of high Cr oxide dispersion strengthened alloys, J. Nucl. Mater. 367-370 (2007) 229–233.
[2] S.A. Briggs, P.D. Edmondson, K.C. Littrell, Y. Yamamoto, R.H. Howard, C.R. Daily, K.A. Terrani, K. Sridharan, K.G. Field, Acta Mater. 129 (2017) 217–228.
[3] A. Kimura, R. Kasada, N. Iwata, H. Kishimoto, C.H. Zhang, J. Isselin, P. Dou, J.H. Lee, N. Muthukumar, T. Okuda, M. Inoue, S. Ukai, S. Ohnuki, T. Fujisawa, T.F. Abe, Development of Al added high-Cr ODS steels for fuel cladding of next generation nuclear systems, J. Nucl. Mater. 417 (2011) 176–179.
[4] J. Isselin, R. Kasada, A. Kimura, Corrosion behaviour of 16%Cr–4%Al and 16%Cr ODS ferritic steels under different metallurgical conditions in a supercritical water environment, Corr. Sci. 52 (2010) 3266–3270.
[5] J. Isselin, R. Kasada, A. Kimura, T. Okuda, M. Inoue, S. Ukai, S. Ohnuki, T. Fujisawa, F. Abe, Evaluation of fracture behavior of recrystallized and aged high-Cr ODS ferritic steels, J. Nucl. Mater. 417 (2011) 185–188.
[6] C.H. Zhang, A. Kimura, R. Kasada, J. Jang, H. Kishimoto, Y.T. Yang, Characterization of the oxide particles in Al-added high-Cr ODS ferritic steels, J. Nucl. Mater 417 (2011) 221–224.
[7] P. Dubuisson, R. Schill, M.P. Hugon, I. Grislin, J.L. Seran, Behavior of an oxide dispersion strengthened ferritic steel irradiated in phenix, Effects of Radiation on Materials: 18th International Symposium, 1325 ASTM STP, 1999, pp. 882–898.
[8] J.F. Ziegler, J.P. Biersack, SRIM 2016 (Stopping and range of ion in materials). Available from: http://www.srim.org.
[9] Y. Dai, S.A. Maloy, G.S. Bauer, W.F. Sommer, Mechanical properties and microstructure in low-activation martensitic steels F82H and ptimax after 800-MeV proton irradiation, J. Nucl. Mater. 283-287 (2000) 513–517.
[10] D.S. Gelles, Neutron irradiation damage in ferritic Fe-Cr alloys, Effects of Radiation on Materials: 14th International Symposium, 1046 ASTM-STP, 1989, p. 73.
[11] S.J. Zincle, Y. Matsukawa, Observation and analysis of defect cluster production and interactions with dislocations, J. Nucl. Mater. 329-333 (2004) 88–96.
[12] C. Deo, C. Tome, R. Lebensohn, S. Maloy, Modeling and simulation of irradiation hardening in structural ferritic steels for advanced nuclear reactors, J. Nucl. Mater. 377 (2008) 136.
[13] J.T. Busby, M.C. Hash, G.S. Was, The relationship between hardness and yield stress in irradiated austenitic and ferritic steels, J. Nucl. Mater. 336 (2005) 267–278.
[14] W.C. Oliver, G.M. Pharr, An improved technique for determining hardness and elastic modulus using load and displacement sensing indentation experiments, J. Mater. Res. 7 (1992) 1564–1583.